Electromagnetically-induced-transparency control of single-atom motion in an optical cavity

Tobias Kampschulte,* Wolfgang Alt, Sebastian Manz, Miguel Martinez-Dorantes, René Reimann, Seokchan Yoon, and Dieter Meschede
Institut für Angewandte Physik, Universität Bonn, Wegelerstraße 8, D-53115 Bonn, Germany

Marc Bienert and Giovanna Morigi
Theoretische Physik, Universität des Saarlandes, D-66123 Saarbrücken, Germany

(Received 31 January 2014; published 4 March 2014)

We demonstrate cooling of the motion of a single neutral atom confined by a dipole trap inside a high-finesse optical resonator. Cooling of the vibrational motion results from electromagnetically induced transparency (EIT)–like interference in an atomic Λ-type configuration, where one transition is strongly coupled to the cavity mode and the other is driven by an external control laser. Good qualitative agreement with the theoretical predictions is found for the explored parameter ranges. Further, we demonstrate EIT cooling of atoms in the dipole trap in free space, reaching the ground state of axial motion. By means of a direct comparison with the cooling inside the resonator, the role of the cavity becomes evident by an additional cooling resonance. These results pave the way towards a controlled interaction among atomic, photonic, and mechanical degrees of freedom.

DOI: 10.1103/PhysRevA.89.033404 PACS number(s): 37.10.De, 37.30.+i, 42.50.Gy

I. INTRODUCTION

Single emitters strongly coupled to optical resonators form a promising basis for the realization of quantum networks [1,2]. Experimental implementations include trapped ions [3], atoms [4–6], artificial superconducting qubits [7], and optomechanical devices [8]. In these platforms, the strong coupling between photons and emitters is utilized to coherently transfer quantum information between stationary qubits at the nodes and flying qubits acting as interconnects. A prerequisite for high-fidelity operations is the control of the coupling with the cavity mode, which implies spatial localization of the emitter at the subwavelength scale. This requirement is easy to fulfill for artificial atoms bound to a substrate. In ion traps the steep confinement puts relatively low requirements on cooling [9–11], while realizations based on neutral atoms in dipole traps (DTs) often require preparation of the motion close to the vibrational ground state. The latter thus calls for efficient cooling techniques, which are robust and sufficiently fast to enable viable quantum technological implementations.

Ground-state cooling of trapped atoms usually makes use of a narrow resonance, which allows one to selectively address transitions where scattering induces the loss of a quantum of vibration [12]. Such resonances can be realized by choosing a suitable dipolar transition, as in sideband cooling. In Raman sideband cooling or electromagnetically-induced-transparency (EIT) cooling, narrow transitions are obtained by coherent two-photon coupling of two stable states [13–17]. One possibility for cooling atoms inside a cavity is to perform Raman sideband cooling there, as shown in Refs. [18] and [19]. The corresponding experimental effort, however, notably increases with the number of degrees of freedom to cool. An alternative is to exploit the strong coupling at the single-photon level. In this case, the relevant narrow resonance is determined by the finite cavity lifetime [20], thus implementing a form of sideband cooling even on dipolar transitions whose radiative linewidth in free space is broader than the trap frequency [21]. In fact, the cavity plays a role similar to that of an additional resonance with linewidth 2κ [22,23]. Sub-Doppler or even subrecoil cooling [24] can then be realized if the cavity linewidth 2κ is smaller than the trap frequency ω. For typical DTs this condition implies rather closed cavities (with a small κ), where coupling photons in and out are relatively slow and which are, thus, less suitable for fast and efficient interfaces.

In this report we experimentally characterize cooling of the vibrational motion of a trapped atom by driving a high-finesse cavity coupled to a three-level Λ transition. This work was triggered by recent experimental studies of single-photon EIT [25,26], where long trap lifetimes have been observed [26], indicating robust cooling in this system, and on recent theoretical studies [27] of cooling in this experimental setup. Here, we demonstrate cavity-assisted EIT cooling of an atom in a DT. The scheme relies on the frequency selectivity of narrow dark resonances, thus the final temperature is not limited by the resolved sideband condition ($2\kappa \ll \omega$). Moreover, we exploit the possibility of switching between EIT-like cooling and cavity cooling by simply changing the detuning of one laser to compare the cooling efficiency in the different regimes, and we show that the interplay of Raman and cavity resonances gives rise to novel and robust cooling regimes. We show that theoretical predictions and experimental results are in remarkable agreement.

II. EXPERIMENTAL SETUP

In our experiment [Fig. 1(a)] single laser-cooled neutral cesium atoms are loaded from a magneto-optical trap (MOT; 852 nm) into a far-red-detuned standing-wave DT (1030 nm) with an axial trap frequency of $\omega_{\mathrm{DT}}/2\pi = 0.3$ MHz along the y direction and a radial trap frequency of about 1 kHz [28]. After verifying that exactly one atom has been loaded and determining its position, it is subsequently transported, using the DT as a conveyor belt, into the mode of the

*kampschulte@uni-bonn.de

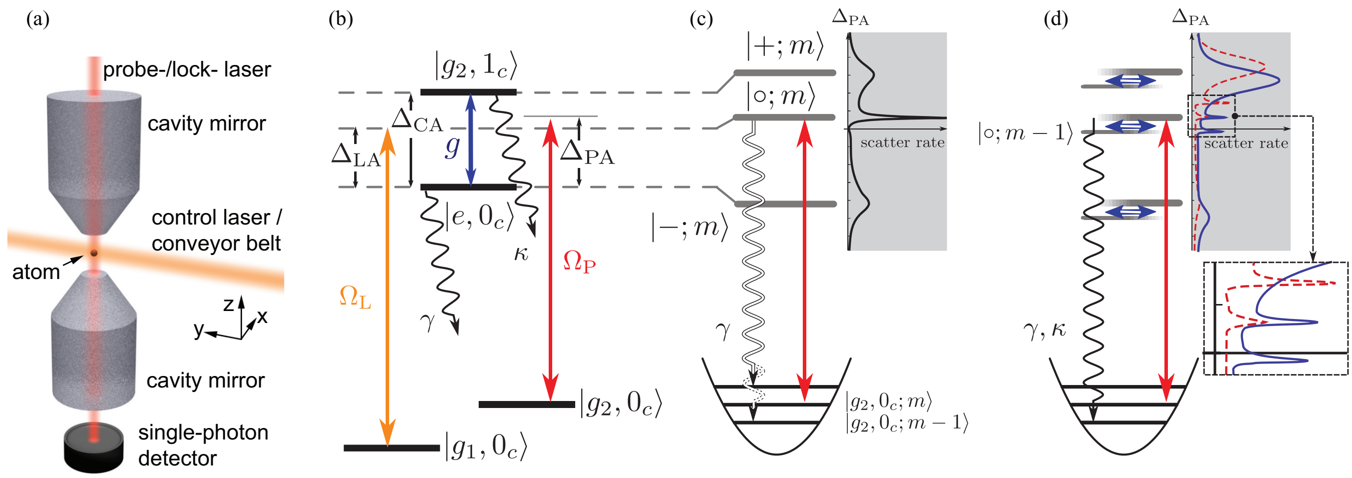

FIG. 1. (Color online) (a) Schematic of the experimental setup. A single cesium atom is trapped inside a high-finesse optical cavity and illuminated by a control laser along the dipole trap axis. A probe laser is coupled into the cavity mode and its transmission is detected by a single-photon detector. (b) Relevant bare energy levels (black) of atom and cavity, Rabi frequencies, and detunings of lasers and cavity mode. (c, d) Dressed states (gray) and scattering processes leading to cooling. Vibrational excitations are shown explicitly. Straight (curvy) arrows represent coherent (incoherent) transitions which lead to a change in energy by one vibrational quantum $\hbar\omega$. Open arrows identify the process which mediates the mechanical action. (c) Cooling (heating) transition due to the recoil of fluorescence photons. Inset: Excitation spectrum, determining the corresponding rate, as a function of the probe frequency. This process is diffusive and can be suppressed using EIT. (d) Cooling transition due to the mechanical effect of the cavity field [horizontal (blue) arrows]. Inset: Corresponding transition rate [solid (blue) curve]. The dashed (red) curve corresponds to heating. The double Fano structure is a consequence of the strong atom-cavity coupling [27]. Diffusion and cooling or heating add up to give the rates $A_\pm^{(j)}$.

high-finesse optical cavity (for details see [29]). The cavity resonance frequency is stabilized using a blue-detuned lock laser (845 nm), which forms, at the same time, a standing-wave DT along the cavity axis and thus confines the atomic motion along the z direction with an axial trap frequency of about $\omega/2\pi = 0.2$ MHz. The relevant electronic levels are the long-lived hyperfine ground states $|g_1\rangle \equiv |6\,^2S_{1/2}, F = 3\rangle$ and $|g_2\rangle \equiv |6\,^2S_{1/2}, F = 4\rangle$, which couple to the common excited state $|e\rangle \equiv |6\,^2P_{3/2}, F = 4\rangle$ via an external control laser (propagating along the y direction) and the cavity mode (along z), respectively. The control laser drives the transition $|g_1\rangle \leftrightarrow |e\rangle$ with effective strength $\Omega_L = 2\pi \times 2.8$ MHz and variable detuning Δ_{LA} [see Fig. 1(b)]. The cavity field has vacuum Rabi frequency $g = 2\pi \times 3.6$ MHz at its antinodes and a detuning of $\Delta_{CA} = 2\pi \times (16 \pm 3)$ MHz from the atomic transition $|g_2\rangle \leftrightarrow |e\rangle$. The cavity is weakly driven by a probe laser with variable detuning Δ_{PA} from the transition $|g_2\rangle \leftrightarrow |e\rangle$. We denote by $\delta_{PC} \equiv \Delta_{PA} - \Delta_{CA}$ its detuning from the empty cavity resonance. At $\delta_{PC} = 0$ the probe-laser strength $\Omega_P = 2\pi \times 0.23$ MHz corresponds to a mean intracavity photon number of 0.08. Since g is larger than the atomic dipole and cavity-field decay rates $(\gamma,\kappa) = 2\pi \times (2.6, 0.40)$ MHz, the system is in the strong-coupling regime, and for our parameters, one atom in state $|g_2\rangle$ causes the cavity transmission to drop by about 50% compared to the on-resonance transmission.

III. THEORETICAL DESCRIPTION

The weak-excitation regime allows us to assume that the relevant states of the cavity field are $|n_c\rangle$, with $n_c = 0,1$ photons. The model for the atom is based on three levels, ignoring that each hyperfine state is degenerate, which will be sufficient to qualitatively describe the experimental results. Therefore, the basis of the atom-photon system consists in states $|g_2,0_c\rangle$, $|g_1,0_c\rangle$, $|e,0_c\rangle$, and $|g_2,1_c\rangle$, which are coupled as depicted in Fig. 1(b). State $|g_2,0_c\rangle$, in particular, weakly couples to state $|g_2,1_c\rangle$, which in turn strongly couples to the other states. The excitation spectrum with respect to the probe laser shows that the level structure is conveniently described in terms of $|g_2,0_c\rangle$, and the dressed states $|\pm\rangle$ and $|\circ\rangle$, i.e., the lowest energy excited eigenstates of the control-laser-driven atom-cavity system neglecting the motion [27] [see Fig. 1(c)]. These dressed states have eigenfrequencies ω_j with $j = \pm,\circ$ and are superpositions of the basis states $|g_1,0_c\rangle$, $|g_2,1_c\rangle$, and $|e,0_c\rangle$. Since the latter two states are radiatively unstable, a finite linewidth γ_j can be associated with each dressed state.

A Fano-like profile is observed [inset in Fig. 1(c)] when the detuning $\delta_{PL} \equiv \Delta_{PA} - \Delta_{LA}$ vanishes, namely, when $|g_2,0_c\rangle$ and $|g_1,0_c\rangle$ are resonantly coupled in a three-stage process: In this case the system exhibits a dark state where $|e,0_c\rangle$ is not excited. Our four-level system is thus similar to the one discussed in [30], whereby here one excitation is purely photonic [27].

An example of scattering processes leading to cooling and heating along the cavity axis is sketched in Fig. 1(c) and 1(d). Setting the probe frequency close to a narrow resonance induces processes where a vibrational quantum can be lost either by a diffusive process associated with the mechanical effect of the flourescence photon [Fig. 1(c)] or by the mechanical force of the cavity field [Fig. 1(d)]. The two kinds of processes add up, giving the total cooling (heating) rate. The existence of dark states leads to Fano resonances in the scattering rates and can be exploited to suppress diffusion and heating processes.

The cooling dynamics is theoretically modeled approximating the dipole potential by a harmonic oscillator and using the rate-equation description in Ref. [27] in a one-dimensional treatment [31]. The model is valid for small photon numbers, $\langle n\rangle \ll 1$, inside the cavity and for weak mechanical coupling, characterized by a small Lamb-Dicke parameter $\eta = [\omega_{\rm rec}/\omega]^{1/2} \ll 1$, where $\omega_{\rm rec}$ is the atomic recoil frequency and ω is the trap frequency. The theory delivers the heating and cooling rates $A_\pm$ connected with photon scattering along the blue and red sideband transitions $|g_2,0_{\rm c},m\rangle \rightarrow |g_2,0_{\rm c},m\pm 1\rangle$, respectively, along the axis of motion. For cooling along the cavity axis (z axis) in the configuration in Fig. 1(a), the rates can be written in the form

$$A_\pm^{(z)} = 2\gamma\mathcal{D} + 2\gamma|\mathcal{T}_\pm^{\gamma,\rm C}|^2 + 2\kappa|\mathcal{T}_\pm^{\kappa,\rm C}|^2. \tag{1}$$

The first term in Eq. (1), proportional to γ and identical for heating and cooling, describes the diffusion of the atomic motion due to mechanical effects of spontaneous decay and corresponds to the process sketched in Fig. 1(c). The second (third) term stems from processes where light is scattered by the atom (cavity), whereby the mechanical action is due to the Jaynes-Cummings coupling [Fig. 1(d)]. The exact form of the quantities $\mathcal{D}$, $\mathcal{T}_\pm^{\gamma,\rm C}$, and $\mathcal{T}_\pm^{\kappa,\rm C}$, and the form of $A_\pm$ for cooling along other directions can be found in [27].

From the quantities $A_\pm$ the cooling rate

$$\Gamma = A_- - A_+, \tag{2}$$

and if $\Gamma > 0$, the mean occupation number

$$\langle m\rangle = \frac{A_+}{A_- - A_+} \tag{3}$$

in the stationary (thermal) state at the end of cooling can be calculated [32]. The cooling rate Γ gives the time scale at which the stationary state of motion is reached.

The general behavior of the rates, (1), is determined by the states $|\pm\rangle,|\circ\rangle$: A_- (A_+) is strongly enhanced whenever the probe laser is resonant with the red (blue) sideband of one of the dressed states, i.e., for $\delta_{\rm PC} = \omega_j - \omega$ ($\delta_{\rm PC} = \omega_j + \omega$). The linewidths γ_j of the dressed states determine the width of these resonances and thereby the cooling dynamics when the probe is tuned to the red sideband. In particular, for $\gamma_j \ll \omega$, resolved sideband cooling at the corresponding dressed-state resonance can be performed.

EIT-like cooling in the cavity can be observed when the resonance condition $\delta_{\rm PC} = \Delta_{\rm LA} - \Delta_{\rm CA}$ is fulfilled. The appearance of a dark state follows from quantum interference among the three dressed states in the excitation process of the cavity-atom system and occurs when the ground state $|g_2,0_{\rm c}\rangle$ is resonantly coupled by three photons (probe, cavity, laser) with $|g_1,0_{\rm c}\rangle$. In this case, the rates are

$$A_\pm^{(z)} = \frac{\Omega_{\rm P}^2/2}{\delta_{\rm PC}^2+\kappa^2}\eta^2\sin^2(kx_0)g^2\gamma \times \frac{1+\mathcal{C}_\pm}{\gamma^2(1+\mathcal{C}_\pm)^2 + \left(\frac{\Omega_{\rm L}^2}{4\omega} - \omega \pm \Delta_{\rm LA} + \frac{\gamma}{\kappa}\mathcal{C}_\pm(\omega\mp\delta_{\rm PC})\right)^2}, \tag{4}$$

with $\mathcal{C}_\pm = C\kappa^2/(\kappa^2 + (\delta_{\rm PC}\mp\omega)^2)$, whereby $C = \tilde{g}^2/(\kappa\gamma)$ is the single-atom cooperativity. The effective coupling constant $\tilde{g} = g\cos kx_0$ is proportional to the vacuum Rabi frequency g at an antinode of the cavity's cosinusoidal mode function of wave number k, with x_0 measuring the distance of the trap center from the antinode. For $\Delta_{\rm LA} = \Delta_{\rm CA}$, three-photon resonance is found for $\delta_{\rm PC} = 0$, and the rates, Eq. (4), take on the form of EIT cooling in free space with a modified Rabi frequency $\Omega_{\rm L}^2 \rightarrow \Omega_{\rm L}^2 + 4\omega^2[\gamma'-\gamma]/\kappa$ and a modified atomic linewidth $\gamma' = \gamma[C\kappa^2/(\kappa^2+\omega^2)+1]$. Hence, due the cavity-boosted Rabi frequency, lower temperatures compared to free-space EIT cooling are possible. Similarly, for large $\delta_{\rm PC}$ (and around $\delta_{\rm PL} = 0$), one recovers normal EIT cooling [13] in a standing wave, where the width of the EIT resonance determines the cooling. For the parameters of the experiment, this sets the limit for the lowest achievable temperatures. To fully enter a regime where quantum interference involving the cavity determines the final vibrational occupation number given by C^{-1}, $\kappa \ll \omega$ is required [27], a condition that is not fulfilled here. Nevertheless, signatures of such a cooling scheme can be found around the range $|\delta_{\rm PC}| \lesssim \omega$, as discussed below.

IV. MEASUREMENTS

Experimentally, the cooling efficiency is characterized by means of the survival probability $P_{\rm s}$, which is measured by first trapping a single atom inside the cavity for a certain holding time t, then retrieving it from the cavity using the conveyor belt, and, finally, detecting its presence by the MOT fluorescence. After many repetitions, the measured $P_{\rm s}$ is given by the ratio between the final and the initial number of atoms. Radiative cooling and heating effects become obvious when we compare $P_{\rm s}$ with the value for atoms in the absence of near-resonant light: In the presence of the far-detuned trapping lasers only (DT and lock laser), $P_{\rm s}$ decays exponentially with a time constant of about 120 ms, limited by parametric heating [33] due to technical intensity fluctuations, mainly of the intracavity lock laser power.

We compare the survival probability with the theoretical predictions for the cooling rate $\Gamma \equiv A_-^{(z)} - A_+^{(z)}$, determining the time scale at which the average number of vibrational excitations along the cavity axis exponentially approaches the stationary value [32]. Figure 2(a) displays a two-dimensional plot of Γ, Eq. (2), using the rates from Eq. (1). Here, the detunings $\delta_{\rm PC}$ and $\Delta_{\rm LA}$ are varied and $\Delta_{\rm CA}$ is at the fixed experimental value. High cooling rates are predicted mostly when the probe laser is tuned to the red side of a dressed-state resonance (shaded areas).

Cooling and heating effects close to the dressed states $|\pm\rangle$, $|\circ\rangle$ become experimentally visible when scanning the probe-cavity detuning $\delta_{\rm PC}$ over a wide range while $\delta_{\rm LC} \equiv \Delta_{\rm LA} - \Delta_{\rm CA} = 0$ remains fixed (dashed-dotted line). Figure 2(b) displays the corresponding survival probabilities $P_{\rm s}$ for two holding times. The heating regions are denoted (i) and (iii). Strong losses in (iii) occur mostly at $\delta_{\rm PC}/2\pi \approx (2\ldots 8)$ MHz, where the laser is tuned on the blue side of the dressed state $|+\rangle$ and heats the motion. In (i) the detuning is $\delta_{\rm PC}/2\pi \approx -25$ MHz and the theory predicts that the motion is outside the Lamb-Dicke regime. The cooling regions are denoted (ii)

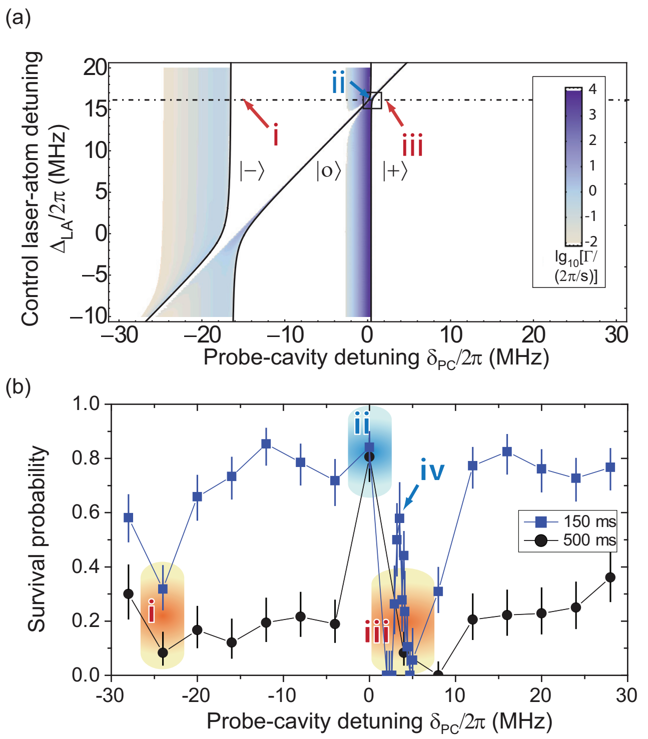

FIG. 2. (Color online) (a) Cooling rate Γ, calculated for a fixed cavity-atom detuning $\Delta_{CA} = 2\pi \times 16$ MHz according to [27]. The horizontal dashed-dotted line corresponds to $\delta_{LC} = 0$. Solid black lines indicate the frequencies of the dressed states $|\pm\rangle, |\circ\rangle$. Away from the avoided crossing at $\delta_{LC} = 0$ the dressed states $|\pm\rangle$ are coherent superpositions of $|g_2, 1_c\rangle$ and $|e, 0_c\rangle$ which are coupled by the cavity field, whereas state $|\circ\rangle$ asymptotically coincides with $|g_1, 0_c\rangle$. Boxed region: Region corresponding to the detail shown in Fig. 3. (b) Measurement of the single-atom survival probability as a function of the probe-cavity detuning δ_{PC} for the case $\delta_{LC} = 0$ and for two holding times t inside the cavity. The parameter space corresponds to the horizontal dashed-dotted line in (a).

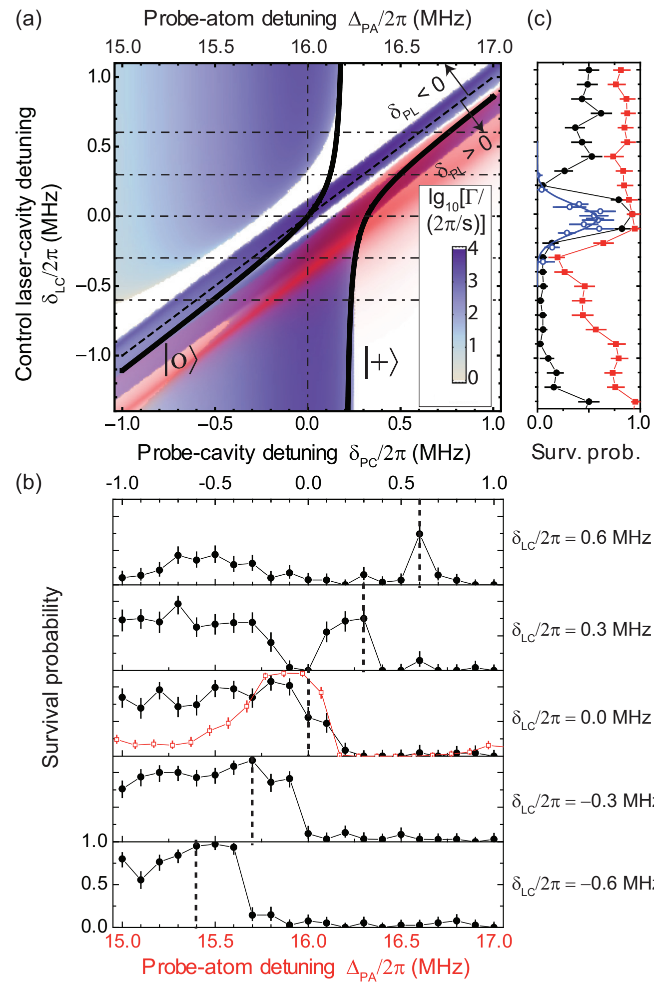

FIG. 3. (Color online) (a) Calculated cooling rate along the cavity axis (blue shading) and heating rate along the control laser axis (red shading). Solid lines indicate the dressed-state energies of $|\circ\rangle$ and $|+\rangle$, while the dashed diagonal line corresponds to $\delta_{PL} = 0$, where $A_\pm$ are given by Eq. (4). Horizontal and vertical dashed-dotted lines correspond to the measurements in (b) and (c), respectively. (b) Survival probability of one atom as a function of the probe-cavity detuning δ_{PC} for five values of δ_{LC} as indicated in (a) for a holding time of $t = 1$ s (black lines). Dashed vertical lines indicate the condition $\delta_{PL} = 0$. For comparison, the lighter (red) line indicates the survival probability as a function of the probe-atom detuning Δ_{PA} for the case of EIT cooling outside the cavity. (c) Survival probability of one atom at probe-cavity resonance $\delta_{PC} = 0$ as a function of δ_{LC} for three holding times: $t = 0.02$, 0.3, and 15 s (red, black, and blue lines, respectively).

and (iv). In (iv), the detuning $\delta_{PC}/2\pi \approx 3.5$ MHz corresponds to the detuning of the orthogonally polarized cavity mode separated by the birefringence splitting, which is not taken into account by the theoretical model. The maximum value of P_s occurs in the narrow region (ii) around $\delta_{PC} = 0$ and $\delta_{PL} = 0$ (see also Ref. [26]).

Figure 3(a) displays a zoom of the behavior of Γ in the boxed region in Fig. 2(a): A rapid change between cooling and heating regions is predicted on the scale of the trapping frequencies. Lowest temperatures are predicted along the diagonal blue stripe at the largest Γ, corresponding to $\delta_{PL} = 0$, with $\langle m_{st}\rangle \approx 0.07$ in the middle and down to 0.05 at the edges of the plot. Moreover, cooling is found in a second diagonal stripe, where $\delta_{PL} \approx \omega$, and in two regions above and below the stripes,where $\delta_{PC} \lesssim 0.2$ MHz $\times\, 2\pi$.

We experimentally verify this behavior by scanning the probe-cavity detuning δ_{PC} over $2\pi \times 2$ MHz (i.e., a few ω_{DT}, ω) around $\delta_{PC} = 0$ for different values of δ_{LC}. The results are displayed in Fig. 3(b): Cooling is found around $\delta_{PL} = 0$. It is also found when the probe laser is resonant or red-detuned from the cavity frequency ($\delta_{PC} \lesssim 0$) and, at the same time, $\delta_{PL} < 0$. Heating occurs for $0 \lesssim \delta_{PL} \lesssim 1$ MHz. This is also shown in Fig. 3(c), where the survival probability as a function of δ_{LC} is displayed [26]. These observations can be understood if we consider that the lifetime of atoms exposed to the lock-laser potential is much shorter than the holding time, hence the atoms only survive if they are cooled along the cavity direction and not heated along the control laser axis. The model predicts heating along this orthogonal axis for $\delta_{PL} > 0$, which is maximum for $\delta_{PL} \approx \omega_{DT}$ [see red shading in Fig. 3(a)]. This could explain the atom losses in this regime and why we see a single cooling peak only at $\delta_{PL} = 0$, corresponding to the upper diagonal stripe. This stripe corresponds to the

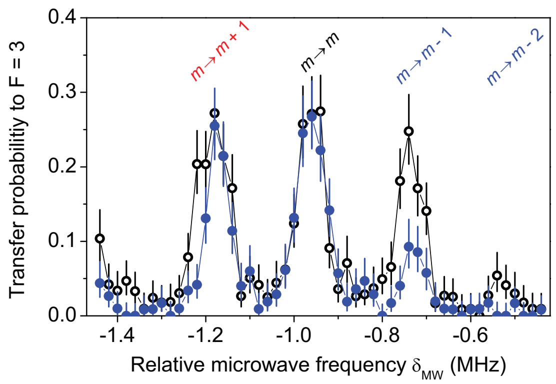

FIG. 4. (Color online) Microwave sideband spectra of EIT-cooled [filled (blue) circles] and molasses-cooled (open black circles) atoms in the standing-wave dipole trap. For this, the cooled atoms were prepared in the Zeeman sublevel $|F = 4, m_F = -4\rangle$ and transferred to $|F = 3, m_F = -3\rangle$ using a microwave pulse of fixed power and duration. The transfer probability was determined by state-selective detection of atoms in $F = 3$ and plotted as a function of the detuning $\delta_{\rm MW}$ of the microwaves from the cesium clock transition frequency. The peak at $\delta_{\rm MW} \approx -1$ MHz corresponds to the carrier transition $m \rightarrow m$. The sideband transitions $m \rightarrow m-1$ and $m \rightarrow m-2$ are strongly reduced in the EIT case, indicating a high occupation of the vibrational ground state.

EIT condition, where cooling is modified due to the presence of the cavity and which is relevant already at the level of a single photon. Interference in the processes of scattering involving the cavity manifests itself in the alternating heating and cooling regions around the EIT stripe and the variation of the cooling rate along the stripe, which, for example, would allow us to efficiently suppress heating transitions if the cavity sidebands were resolved. We denote this mechanism cavity-assisted EIT (CEIT) cooling. The cooling at $\delta_{\rm PC} \lesssim 0$, instead, is based on the excitation of the red sideband of the cavity-like dressed state $|+\rangle$ [22,34]. Here, in the limit of large $|\delta_{\rm PL}|$, the control laser acts like an incoherent repumper that transfers atoms that decay into state $|g_1\rangle$ and back to state $|g_2\rangle$, and the system can be treated as an effective two-level system [23,26].

In order to clarify the role of the cavity in CEIT cooling, we compare the observed dynamics with EIT cooling in free space. For this purpose we measure the survival probability with small ensembles of atoms trapped in the standing-wave DT outside the cavity (at the position of the MOT). Here, the probe laser ($\Omega_{\rm p}/2\pi = 0.5$ MHz) is directly shone on the atoms, which are strongly confined only along the control-laser axis. The holding time of 300 ms is much shorter than the trap lifetime of several seconds. The atoms only survive within a narrow region around $\delta_{\rm PL} = 0$ (EIT condition) [see the middle plot in Fig. 3(b)].

To quantify the performance of EIT cooling in the DT and to compare it with standard molasses cooling, we apply microwave sideband spectroscopy by making the lattice slightly state dependent [35]. Figure 4 shows spectra taken with EIT- and molasses-cooled atoms, respectively. The significant reduction in the $m \rightarrow m-1$ and $m \rightarrow m-2$ sideband transitions compared to the $m \rightarrow m+1$ transition indicates already a high population in the ground state of axial motion (along y) for the EIT-cooled atoms. In performing robust adiabatic passages on the $m \rightarrow m-1$ transition, we infer, for the EIT-cooled (molasses-cooled) atoms, a steady-state temperature of $7.0 \pm 0.5\ \mu$K ($31 \pm 6\ \mu$K), corresponding to a final ground-state occupation of 0.78 ± 0.02 (0.29 ± 0.05), respectively. From the variation in the duration of the EIT cooling, a cooling rate of about 1 kHz has been inferred, compatible with predictions in Ref. [15].

V. DISCUSSION

With our setup we have successfully demonstrated EIT cooling applied to neutral atoms in a DT. When comparing the measurement of the survival probability with the corresponding one in the presence of the resonator, there is an obvious difference on the red side ($\delta_{\rm PL} < 0$) of the EIT condition. This is because the cavity adds a new resonance, extending the cooling region to a larger range of probe-cavity detunings $\delta_{\rm PC}$, thereby making the cooling more robust. For this reason, these dynamics are also suitable for simultaneously cooling several degrees of freedom, for instance, atomic arrays [17,36]. Moreover, as shown in Fig. 3(b), in CEIT different cooling profiles can be achieved by changing $\delta_{\rm LC}$, reflecting the additional interference effect and resonance, which are absent in free space.

In conclusion, this work has investigated a scheme of CEIT cooling and provides a comparison between the efficiency of free-space cooling and that of cavity cooling. These techniques can be extended for cooling optomechanical systems [37] coupled to a single emitter [38]. Our setup, moreover, can serve as a transducer among the vibrational, electronic, and photonic degrees of freedom, thereby realizing a continuous-variable quantum interface with single atoms [39].

ACKNOWLEDGMENTS

The authors acknowledge discussions with J. Eschner and D. Leibfried and financial support from BMBF (QuOReP), the European Commission (IP SIQS, ITN CCQED, STREP PICC), and the German Research Foundation (DFG). R.R. and S.M. acknowledge financial support from the Studienstiftung des deutschen Volkes. M.D., R.R., and S.M. acknowledge financial support from the BCGS.

[1] J. I. Cirac, P. Zoller, H. J. Kimble, and H. Mabuchi, Phys. Rev. Lett. **78**, 3221 (1997).
[2] H. J. Kimble, Nature **453**, 1023 (2008).
[3] A. Stute, B. Casabone, P. Schindler, T. Monz, P. O. Schmidt, B. Brandstätter, T. E. Northup, and R. Blatt, Nature **485**, 482 (2012).

[4] R. Miller, T. E. Northup, K. M. Birnbaum, A. Boca, A. D. Boozer, and H. J. Kimble, J. Phys. B **38**, S551 (2005).
[5] T. Wilk, S. C. Webster, A. Kuhn, and G. Rempe, Science **317**, 488 (2007).
[6] S. Ritter, C. Nölleke, C. Hahn, A. Reiserer, A. Neuzner, M. Uphoff, M. Mücke, E. Figueroa, J. Bochmann, and G. Rempe, Nature **484**, 195 (2012).
[7] A. Wallraff, D. I. Schuster, A. Blais, L. Frunzio, R.-S. Huang, J. Majer, S. Kumar, S. M. Girvin, and R. J. Schoelkopf, Nature **431**, 162 (2004).
[8] E. Verhagen, S. Deleglise, S. Weis, A. Schliesser, and T. J. Kippenberg, Nature **482**, 63 (2012).
[9] G. R. Guthörlein, M. Keller, K. Hayasaka, W. Lange, and H. Walther, Nature **414**, 49 (2001).
[10] A. B. Mundt, A. Kreuter, C. Becher, D. Leibfried, J. Eschner, F. Schmidt-Kaler, and R. Blatt, Phys. Rev. Lett. **89**, 103001 (2002).
[11] M. Keller, B. Lange, K. Hayasaka, W. Lange, and H. Walther, Nature **431**, 1075 (2004).
[12] J. Eschner, G. Morigi, F. Schmidt-Kaler, and R. Blatt, J. Opt. Soc. Am. B **20**, 1003 (2003).
[13] G. Morigi, J. Eschner, and C. H. Keitel, Phys. Rev. Lett. **85**, 4458 (2000).
[14] C. F. Roos, D. Leibfried, A. Mundt, F. Schmidt-Kaler, J. Eschner, and R. Blatt, Phys. Rev. Lett. **85**, 5547 (2000).
[15] G. Morigi, Phys. Rev. A **67**, 033402 (2003).
[16] F. Schmidt-Kaler, J. Eschner, G. Morigi, C. Roos, D. Leibfried, A. Mundt, and R. Blatt, Appl. Phys. B **73**, 807 (2001).
[17] Y. Lin, J. P. Gaebler, T. R. Tan, R. Bowler, J. D. Jost, D. Leibfried, and D. J. Wineland, Phys. Rev. Lett. **110**, 153002 (2013).
[18] A. D. Boozer, A. Boca, R. Miller, T. E. Northup, and H. J. Kimble, Phys. Rev. Lett. **97**, 083602 (2006).
[19] A. Reiserer, C. Nölleke, S. Ritter, and G. Rempe, Phys. Rev. Lett. **110**, 223003 (2013).
[20] V. Vuletić, H. W. Chan, and A. T. Black, Phys. Rev. A **64**, 033405 (2001).
[21] D. R. Leibrandt, J. Labaziewicz, V. Vuletić, and I. L. Chuang, Phys. Rev. Lett. **103**, 103001 (2009).
[22] S. Zippilli and G. Morigi, Phys. Rev. A **72**, 053408 (2005).
[23] M. Bienert and G. Morigi, Phys. Rev. A **86**, 053402 (2012).
[24] M. Wolke, J. Klinner, H. Keßler, and A. Hemmerich, Science **337**, 75 (2012).
[25] M. Mücke, E. Figueroa, J. Bochmann, C. Hahn, K. Murr, S. Ritter, C. J. Villas-Boas, and G. Rempe, Nature **465**, 755 (2010).
[26] T. Kampschulte, W. Alt, S. Brakhane, M. Eckstein, R. Reimann, A. Widera, and D. Meschede, Phys. Rev. Lett. **105**, 153603 (2010).
[27] M. Bienert and G. Morigi, New J. Phys. **14**, 023002 (2012).
[28] The weak radial confinement allows for a slow variation of the atom-cavity coupling strength; see Ref. [29] .
[29] M. Khudaverdyan, W. Alt, I. Dotsenko, T. Kampschulte, K. Lenhard, A. Rauschenbeutel, S. Reick, K. Schörner, A. Widera, and D. Meschede, New J. Phys. **10**, 073023 (2008).
[30] C. Champenois, G. Morigi, and J. Eschner, Phys. Rev. A **74**, 053404 (2006).
[31] Within the Lamb-Dicke limit, no coupling between different spatial directions is present. Hence, the cooling along the traps in the z and y directions can be described independently .
[32] S. Stenholm, Rev. Mod. Phys. **58**, 699 (1986).
[33] M. E. Gehm, K. M. O'Hara, T. A. Savard, and J. E. Thomas, Phys. Rev. A **58**, 3914 (1998).
[34] P. Domokos and H. Ritsch, J. Opt. Soc. Am. B **20**, 1098 (2003).
[35] L. Förster, M. Karski, J.-M. Choi, A. Steffen, W. Alt, D. Meschede, A. Widera, E. Montano, J. H. Lee, W. Rakreungdet, and P. S. Jessen, Phys. Rev. Lett. **103**, 233001 (2009).
[36] M. H. Schleier-Smith, I. D. Leroux, H. Zhang, M. A. Van Camp, and V. Vuletić, Phys. Rev. Lett. **107**, 143005 (2011).
[37] See, for example, T. J. Kippenberg and K. J. Vahala, Science **321**, 1172 (2008), and references therein; J. Chan, T. P. Mayer Alegre, A. H. Safavi-Naeini, J. T. Hill, A. Krause, S. Gröblacher, M. Aspelmeyer, and O. Painter, Nature **478**, 89 (2011).
[38] D. Breyer and M. Bienert, Phys. Rev. A **86**, 053819 (2012).
[39] A. S. Parkins and H. J. Kimble, J. Opt. B **1**, 496 (1999).